Inhibition of centromere dynamics by eribulin (E7389) during mitotic metaphase

Tatiana Okouneva,[1] Olga Azarenko,[1] Leslie Wilson,[1] Bruce A. Littlefield,[2] and Mary Ann Jordan[1]

[1]Department of Molecular, Cellular, and Developmental Biology and Neuroscience Research Institute, University of California Santa Barbara, Santa Barbara, California and [2]Eisai Research Institute, Andover, Massachusetts

Abstract

Eribulin (E7389), a synthetic analogue of halichondrin B in phase III clinical trials for breast cancer, binds to tubulin and microtubules. At low concentrations, it suppresses the growth phase of microtubule dynamic instability in interphase cells, arrests mitosis, and induces apoptosis, suggesting that suppression of spindle microtubule dynamics induces mitotic arrest. To further test this hypothesis, we measured the effects of eribulin on dynamics of centromeres and their attached kinetochore microtubules by time-lapse confocal microscopy in living mitotic U-2 OS human osteosarcoma cells. Green fluorescent protein–labeled centromere-binding protein B marked centromeres and kinetochore-microtubule plus-ends. In control cells, sister chromatid centromere pairs alternated under tension between increasing and decreasing separation (stretching and relaxing). Eribulin suppressed centromere dynamics at concentrations that arrest mitosis. At 60 nmol/L eribulin (2 × mitotic IC_{50}), the relaxation rate was suppressed 21%, the time spent paused increased 67%, and dynamicity decreased 35% (but without reduction in mean centromere separation), indicating that eribulin decreased normal microtubule-dependent spindle tension at the kinetochores, preventing the signal for mitotic checkpoint passage. We also examined a more potent, but in tumors less efficacious antiproliferative halichondrin derivative, ER-076349. At 2 × IC_{50} (4 nmol/L), mitotic arrest also occurred in concert with suppressed centromere dynamics. Although media IC_{50} values differed 15-fold between the two compounds, the intracellular concentrations were similar, indicating more extensive relative uptake of ER-076349 into cells compared with eribulin. The strong correlation between suppression of kinetochore-microtubule dynamics and mitotic arrest indicates that the primary mechanism by which eribulin blocks mitosis is suppression of spindle microtubule dynamics. [Mol Cancer Ther 2008;7(7):2003–11]

Introduction

Eribulin (E7389, a synthetic derivative of the natural product halichondrin B; Fig. 1) is a microtubule-targeted drug that inhibits cancer cell proliferation at nanomolar concentrations. It is currently in phase III clinical trials. We found previously that eribulin binds to tubulin and suppresses microtubule dynamics, both *in vitro* and in cells, by a unique mechanism that involves suppression of the growth phase of microtubule dynamic instability without suppressing shortening (1). Suppression of microtubule dynamics in interphase cells occurs at eribulin concentrations that arrest mitosis and lead to apoptosis (1–4). An important question, however, is whether eribulin suppresses microtubule dynamics in mitotic cells, leading to mitotic arrest, and if so, how are the dynamics suppressed. To address this question, in the present study, we used human osteosarcoma (U-2 OS) cells whose chromosomal centromeres were labeled with green fluorescent protein (GFP)–labeled CENP-B to examine the effects of eribulin on the movements of centromeres and their associated dynamic microtubules during mitotic arrest. We also extended our examination of the mechanism of action of this class of compounds by comparing the effects of eribulin with those of ER-076349, a halichondrin analogue that is a more potent antiproliferative agent in cells, albeit less effective against tumors in *in vivo* xenograft models.

During mitosis, the forces generated by the mitotic spindle are translated into chromosomal movement mainly through the interaction of the spindle microtubules with kinetochores. Kinetochores are specialized protein complexes that assemble at the centromeres of chromosomes at mitosis. During metaphase, the duplicated chromosomes with their centromere/kinetochore-attached microtubules align at the metaphase plate with the sister centromeres remaining attached, and the chromosome pairs continue to undergo complex movements. The individual chromosome pairs oscillate independently toward and away from the spindle poles. In addition, the two kinetochores of each pair repeatedly separate from each other (they stretch apart) and then return to a relaxed position (5, 6). The plus-ends of spindle kinetochore microtubules are embedded in the kinetochore/centromere complex; thus, kinetochore microtubules are a major force inducing centromere dynamics, and centromere dynamics provide a readout of spindle microtubule dynamics.

Received 1/28/08; revised 4/25/08; accepted 5/7/08.

Grant support: Eisai Research Institute and NIH grant CA 57291.

The costs of publication of this article were defrayed in part by the payment of page charges. This article must therefore be hereby marked *advertisement* in accordance with 18 U.S.C. Section 1734 solely to indicate this fact.

Requests for reprints: Mary Ann Jordan, Department of Molecular, Cellular, and Developmental Biology and Neuroscience Research Institute, University of California Santa Barbara, Santa Barbara, CA 93106. Phone: 805-893-5317; Fax: 805-893-4724. E-mail: jordan@lifesci.ucsb.edu

doi:10.1158/1535-7163.MCT-08-0095

Dynamic microtubules and microtubule-based motor proteins produce tension on kinetochores, which plays an important role in fulfilling the mitotic spindle checkpoint and inducing passage from metaphase to anaphase (5–8). The spindle checkpoint is essential for ensuring the accurate segregation of a complete set of chromosomes to each daughter cell (reviewed in ref. 9). It ensures that segregation is delayed until all chromosomes are properly attached to a bipolar spindle. The checkpoint monitors attachment of the proper number of microtubules to the kinetochores and tension on the kinetochores, and the two aspects may be interdependent because tension stabilizes and increases the number of kinetochore microtubule attachments (10, 11). The dynamic connection between kinetochores and microtubules results in activation of a signal transduction network consisting of Mad, Bub, and Mps1 protein that regulates anaphase entry by acting on the anaphase-promoting complex that in turn targets the anaphase-inhibitory protein securin for destruction. However, how tension is sensed by the kinetochores and how the kinetochore transmits its inhibitory signals are unknown (9).

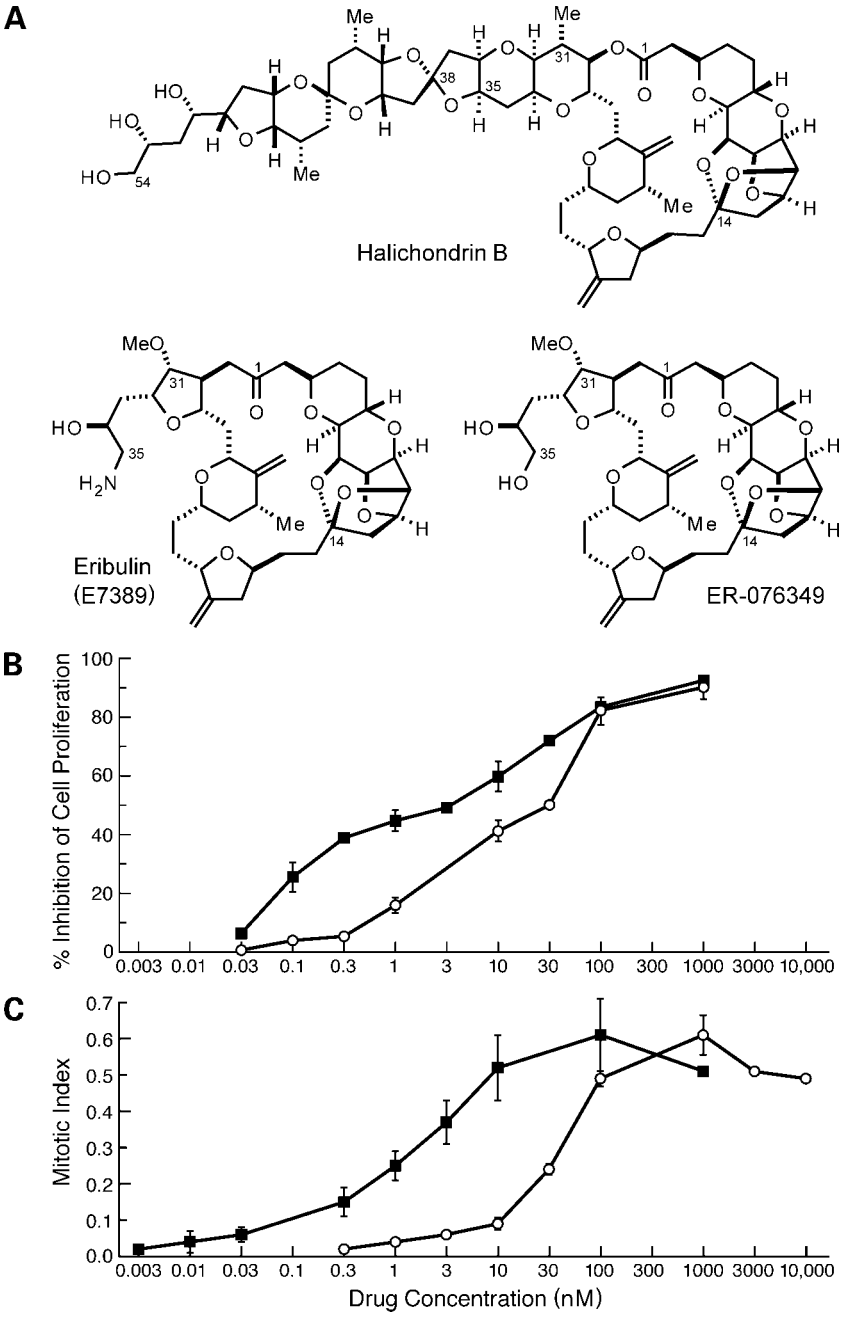

Figure 1. **A,** structures of halichondrin B, eribulin, and ER-076349. **B,** inhibition of proliferation of U-2 OS human osteosarcoma cells by eribulin (*circles*) and ER-076349 (*squares*). Cell proliferation was determined by counting live cells at the time of drug addition and 28 h later. IC_{50}, eribulin, 30 nmol/L; ER-076349, 3 nmol/L. **C,** accumulation of cells in mitosis after incubation with eribulin (*circles*) and ER-076349 (*squares*). Mitotic accumulation was determined by counting cells by microscopy following fixation and staining of microtubules and chromatin. Half-maximal mitotic arrest occurred at 30 nmol/L for eribulin and at 2 nmol/L for ER-076349. Mean and SE of five independent experiments.

Here, we found that both eribulin and ER-076349 significantly reduced centromere stretching and relaxation at concentrations that arrest mitosis. Interestingly, the reduction in dynamics occurred without a concomitant reduction in the centromere separation distance. Although the IC_{50} values for inhibition of mitosis and proliferation differ 10- to 15-fold for the two compounds, the intracellular concentrations of eribulin and ER-076349 that resulted in mitotic arrest and suppressed centromere dynamics were nearly identical to each other, suggesting that the two drugs have common intracellular targets and similar binding affinities for microtubules and actions on mitotic arrest. The results indicate that suppression of mitotic spindle microtubule dynamics is the mechanism by which eribulin and ER-076349 inhibit mitosis. They also confirm and extend previous results with paclitaxel and *Vinca* alkaloids, indicating that suppression of spindle microtubule dynamics is the major mechanism of mitotic arrest by chemically dissimilar microtubule poisons (12, 13).

Materials and Methods

Materials

Unlabeled and tritium-labeled eribulin (NSC 707389; formerly E7389; distinguished by C35-amine) and ER-076349 (C35-hydroxy analogue), macrocyclic ketone analogues of the marine sponge natural product halichondrin B (4), were synthesized at Eisai Research Institute (14). Structures of both analogues and parental halichondrin B are presented in Fig. 1A.

Cell Culture

U-2 OS human osteosarcoma cells (American Type Culture Collection) were maintained in DMEM supplemented with 1% penicillin-streptomycin, nonessential amino acids (Sigma), and 10% fetal bovine serum (Hyclone) in 250 mL tissue culture flasks or 35 mm six-well plates (Falcon, Becton Dickinson) at 37°C in a 5% CO_2 atmosphere; doubling time was 28 h. Cells were stably transfected with a CENP-B-GFP plasmid containing the coding region for the DNA-binding domain of CENP-B (codons 1-167) fused to the amino terminus of the *A. victoria* GFP cDNA as described previously (5). Expression of GFP-CENP-B was stable for 8 to 10 weeks as determined by fluorescence microscopy.

Cell Proliferation and Mitotic Index

Cells were seeded on poly-L-lysine-treated (50 mg/mL, 2 h, 37°C, washed once with sterile water) sterile glass coverslips in six-well plates at 1×10^5 cells per 2 mL/well. One day later, medium was replaced with fresh medium containing a range of eribulin or ER-076349 concentrations (0.003-10,000 nmol/L) and further incubated for one cell cycle (28 h). Cells were harvested by combining floating cells with attached cells, which had been released by trypsinization [0.5 mg/mL in PBS: 137 mmol/L NaCl, 2.7 mmol/L KCl, 1.5 mmol/L KH_2PO_4, 8.1 mmol/L Na_2HPO_4, 0.5 mmol/L EDTA (pH 7.2); 5 min, 37°C] and live cells were counted using a hemacytometer. Trypan blue dye was used to distinguish living from dead cells. To evaluate mitotic indices, cells were grown for 20 h in the absence and presence of drug. Mitotic indices were determined by microscopic examination of chromosomes and GFP-CENP-B centromeres in cells that were fixed in formalin/methanol (described below), stained with 4,6′-diamidino-2-phenylindole, and imaged using a Nikon Eclipse E800 microscope with ×60 and ×100 (numerical aperture 1.4 for both) objectives. Results are the mean and SE of five independent experiments, in which a minimum of 1,000 cells were counted for each condition in each experiment. IC_{50} values were determined by linear regression of double-reciprocal plots of proliferation or mitotic index versus drug concentration.

Immunofluorescence Microscopy

Immunofluorescence localization of microtubules and chromosomes was done on cells that were fixed in 10% formalin in PBS (20 min, 25°C) followed by 10 min in methanol (4°C), washed three times with PBS, and incubated for 30 min with 1% normal goat serum (Sigma) to avoid nonspecific binding. Cells were incubated with mouse monoclonal anti-tubulin antibodies (DM1A + DM1B, Abcam; 1:1,000; 1 h, 37°C). Cells were rinsed three times in PBS containing 1% bovine serum albumin and incubated with goat anti-mouse CY3-conjugated secondary antibody (Jackson ImmunoResearch Laboratories; 1:1,000; 1 h, 37°C). Cells were rinsed three times in PBS-bovine serum albumin, mounted with Prolong Antifade (Molecular Probes), and imaged as above.

Imaging Centromeres in Living Cells

Following incubation with or without drugs for 4 h, poly-L-lysine-coated coverslips with live cells attached were mounted in a Dvorak-Stotler chamber (Nicholson Precision Instruments) in the medium in which they had been cultured (with or without drug) and maintained on the microscope stage at 37°C in a Lucite box. Images of live cells were collected on a Nikon Diaphot 200 inverted confocal microscope with a ×100 Nikon PlanApo lens with a 7× zoom at 3% to 10% laser power. Pairs of fluorescent centromeres were easily identified because as cells enter mitosis, spindles and centromere pairs align parallel to the substrate. Each time course consisted of a series of 120 single images (2 Kalman images each) at 5 s intervals (total time 10 min) at slow scan speed and were collected at 128 × 128 pixel box size (each pixel was 0.1 μm). In each time course, several centromere pairs could be distinguished and followed.

Image Processing and Quantitative Motility Analysis

Time-lapse image sequences were viewed as movies using Bio-Rad Confocal Assistant Software 4.01 to identify centromere pairs that could be tracked through the sequence for at least 8 min (96 frames). Image stacks were then imported into MetaMorph (version 4.6) imaging software (Universal Imaging) for analysis. The x-y position assigned to a centromere was determined by the brightest pixel at the center of the fluorescent signal. Its position and the distance from the sister centromere were recorded on an Excel spreadsheet (Microsoft). The series of separation distances was used to determine rates of separation

(stretching) and coming together (relaxing), the durations of these movements, and the frequencies of transition from stretching to relaxing and vice versa.

Background Motion

Centromere movement attributable to simple diffusion or electronic noise rather than to microtubule dynamics and/or motor proteins was determined previously to be 0.34 μm/min, the mean rate of movement in the absence of microtubules (13). Any movement less than this was considered to be background or diffusion movement and classified as a ''pause'' or a movement that was so attenuated that it could not be reliably measured.

Selection of Centromere Pairs for Measurement of Dynamics

For determination of centromere dynamics, only cells in which the majority of chromosomes had congressed to a well-formed and distinct bipolar metaphase plate were measured and only centromere pairs of congressed chromosomes were included. At high drug concentrations, ~80% of spindles were abnormal (mostly multipolar), and many chromosomes had not congressed.

Intracellular Drug Concentration

U-2 OS cells were seeded into poly-L-lysine-treated scintillation vials (1×10^5 cells, 2 mL). After 24 h, medium was replaced with fresh medium containing 30 to 60 nmol/L [^{3}H]eribulin (final specific activity after dilution with unlabeled eribulin: 2 mCi/mol) or 2 to 4 nmol/L [^{3}H]ER-076349 (final specific activity: 18-24 mCi/mol) or unlabeled drug (for determination of cell number). Medium was removed from vials from 30 min to 20 h after drug addition, cells were rapidly rinsed twice with 2 mL PBS, and intracellular drug concentration was determined by scintillation counting. Background radioactivity was determined after washing vials that contained only radiolabeled drug in medium. Cell number was determined by manual cell counting using a hemacytometer at the time of drug addition and 20 h later in vials treated in parallel using unlabeled drug. The intracellular drug concentration was determined by dividing the moles of intracellular eribulin by the average cell volume times the number of cells per vial. The mean cell volume was calculated from the mean diameter of cells rounded up after trypsinization (n = 38; mean cell volume, 3.2×10^{-12} L). Additionally, after 20 h, cells were washed with 2 mL PBS and fresh medium was added for 1 and 24 h to determine how readily the drugs are washed out of cells. All time points were measured in duplicate, and results are the mean and SE of five experiments.

Results

Effects of Eribulin and ER-076349 on Mitosis in U-2 OS Cells

The goal of these experiments was to measure the movements of centromeres due to the growing and shortening dynamics of their attached dynamic microtubules in living U-2 OS human osteosarcoma cells at drug concentrations that inhibited proliferation and arrested mitosis. Thus, we first determined the effects of eribulin and ER-076349 on cell proliferation (28 h, one cell cycle) and mitotic progression. Cell proliferation was inhibited with IC_{50} values of 30 nmol/L eribulin and 3 nmol/L ER-076349 (Fig. 1B).

The effects of the drugs on mitotic progression were measured by incubating the cells with drug (3 pmol/L to 10 μmol/L, 20 h) and determining the mitotic index by microscopy (Materials and Methods). At concentrations >3 nmol/L for eribulin and >0.1 nmol/L for ER-076349, cells accumulated in mitosis reaching a maximum of 60% at 1 μmol/L eribulin and at 100 nmol/L ER-076349 (Fig. 1C). Half-maximal arrest occurred at 30 nmol/L eribulin and at 2 nmol/L ER-076349, nearly the same as the IC_{50} values observed for proliferation. ER-076349 was thus 15 times more potent than eribulin in U-2 OS cells.

Spindle and Microtubule Organization and Localization of GFP-CENP-B

The localization of GFP-CENP-B, microtubules, and chromosomes in the presence and absence of drugs (4 h incubation) is shown in fixed and immunostained U-2 OS cells in Fig. 2A to D. In control cells at metaphase (Fig. 2A), chromosomes were completely congressed to the metaphase plate, and centromere pairs (*arrows*) were oriented parallel to the spindle axis. During anaphase, sister chromatids and their associated centromeres separated and the centromeres appeared as single, spherical dots (Fig. 2B). After 4 h incubation with 30 nmol/L eribulin or 2 nmol/L ER-076349, spindles were somewhat smaller but were often bipolar with all chromosomes congressed to the metaphase plate. However, many spindles were bipolar but with ''lagging'' chromosomes or chromosomes stuck at one or both poles (Fig. 2C, *arrow*). Some spindles were tripolar or multipolar (Fig. 2D).

Dynamic Behavior of Centromeres in Living Cells

Attached sister centromeres, as observed by confocal microscopy in metaphase cells, undergo alternating phases of increasing and decreasing separation, referred to as ''stretching'' and ''relaxing.'' The behavior of a typical pair of centromeres in a control cell during a period of 480 s is shown in Fig. 2E to H (*arrows*). At zero time, the sister centromeres (*arrows*) are separated by 0.9 μm in Fig. 2E, by 0.7 μm in Fig. 2F (at 70 s), by 1.2 μm in Fig. 2G (at 225 s), and by 0.6 μm in Fig. 2H (at 260 s).

Figure 3A and B represents a time course of stretching and relaxing of a pair of sister centromeres, determined from images like those shown in Fig. 2. The upper trace (Fig. 3A) shows the distance between the two members of a centromere pair in a control cell and the lower trace is the distance between the two members of a pair in the presence of 60 nmol/L eribulin. These plots, which are analogous to ''life history'' plots showing microtubule growth and shortening dynamics (15), were used to determine the variables of sister centromere stretching and relaxing dynamics. Centromeres stretched apart during microtubule shortening phases and relaxed back together during microtubule growing phases. For some periods, pairs underwent little or no detectable change in separation

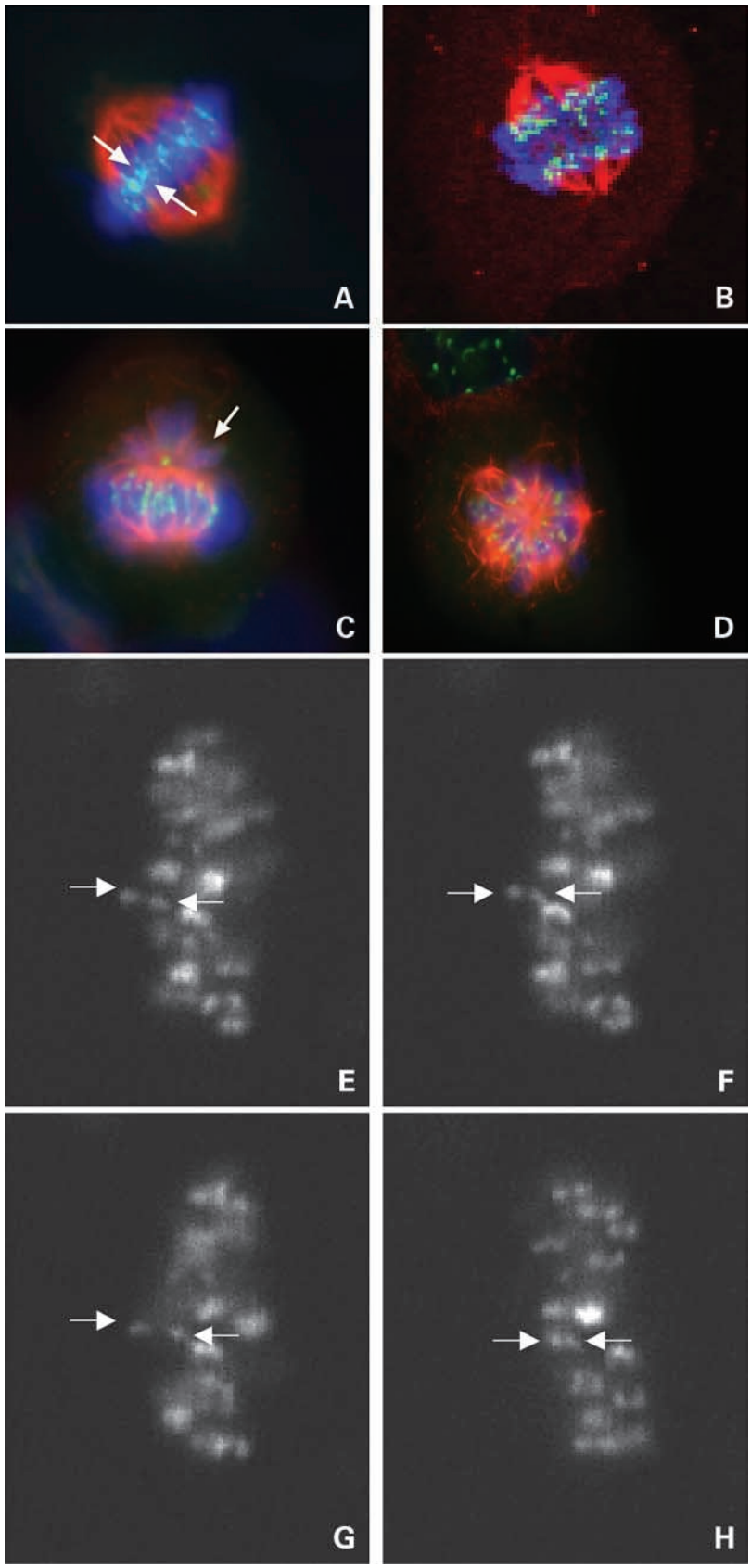

Figure 2. **A** to **D,** centromeres, microtubules, and chromosomes in U-2 OS cells in the absence (**A** and **B**) or presence (**C** and **D**) of eribulin. Cells expressing GFP-CENP-B (*green*) were incubated with or without eribulin (28 h), fixed, and stained with antibody to α-tubulin (*red*) and with 4,6′-diamidino-2-phenylindole for chromosomes. In control cells in metaphase (**A**), pairs of sister centromeres are present on sister chromatids and are separated by variable distance. In anaphase (**B**), sister chromatids and centromeres have separated. At half-maximal mitotic arrest 30 nmol/L eribulin (**C** and **D**) and 2 nmol/L ER-076349 (data not shown), spindles were abnormal bipolar with uncongressed chromosomes (*arrow*; **C**) or multipolar (**D**). At 60 nmol/L eribulin or 4 nmol/L ER-076349, most spindles were multipolar. **E** to **H,** dynamic behavior of centromeres in living U-2 OS cells in the absence of drug. Images of GFP centromeres were collected from a single plane by confocal microscopy at 5 s intervals. *Arrowheads,* positions of sister centromeres at time 50 s (separated by 0.93 μm; **E**); in the second (**F**), third (**G**), and fourth (**H**) panels (120, 275, and 310 s), they are separated by 0.70, 1.2, and 0.59 μm.

distance, called a ''pause,'' or a period in which movement was not significantly different from background movement measured in the absence of microtubules (0.34 μm/min; Materials and Methods). In the presence of 60 nmol/L eribulin (Fig. 3B), the amplitude of centromere separations was significantly reduced.

Centromere Dynamics in Control U-2 OS cells

The variables of centromere dynamics are shown in Table 1. In the absence of drug, the relaxation rate of centromere pairs was faster than the stretching rate (1.4 ± 0.5 and 1.0 ± 0.4 μm/min, respectively; Table 1). The mean separation distance was 0.66 ± 0.11 μm, with a mean maximum separation distance of 0.96 ± 0.11 μm and a mean minimum separation distance of 0.45 ± 0.12 μm (Table 1). Centromere pairs in control cells spent 38 ± 2% of the time stretching, 32 ± 2% of the time relaxing, and 30 ± 3% of the time in a paused state. The overall rate of centromere stretching and relaxation, the ''dynamicity'' (analogous to the term as used in describing microtubule dynamics; ref. 16) is the sum of the distances moved during stretching and relaxation divided by the total time in all phases. The centromere dynamicity in the absence of drugs was 0.84 μm/min.

Effects of Eribulin and ER-076349 on Centromere Dynamics

We examined centromere dynamics at the mitotic IC_{50} and twice the mitotic IC_{50} for both compounds (30 and 60 nmol/L eribulin and 2 and 4 nmol/L ER-076349) after incubation with drug for 4 h. As shown in Table 1, both drugs suppressed centromere dynamics at concentrations that arrested mitosis. The most prominent and concentration-dependent changes were reductions in the percentages of time spent stretching and relaxing, increases in the percentage of time spent in a paused state, and suppression of the overall dynamicity (by 6% and 35% for 30 and 60 nmol/L eribulin, respectively, and by 5% and 32% by 2 and 4 nmol/L ER-076349, respectively; Table 1). Although effects on the stretching rate were minimal, both compounds significantly suppressed the relaxing rate by 21% at 2 × IC_{50}. The transition frequency was not affected at the IC_{50} but was reduced at 2 × IC_{50} (by 24% and 35% for eribulin and ER-076349, respectively). In contrast with the effects of vinblastine and paclitaxel on centromere dynamics (12, 13), eribulin and ER-076349 had no significant effect on the mean separation distance.

Intracellular Levels of Eribulin and ER-076349

The time courses for uptake of eribulin and ER-076349 into U-2 OS cells at their IC_{50} and 2 × IC_{50} values are shown in Fig. 4. Eribulin (30 and 60 nmol/L) was taken up rapidly into the cells, attaining intracellular concentrations of 1 and 3.5 μmol/L, respectively, 4 h after addition, and remaining at approximately those levels at least to 20 h. Thus eribulin accumulated in the cells 30- to 60-fold over its concentration in the medium. ER-076349 (2 and 4 nmol/L) was taken up more rapidly, attaining intracellular concentrations of 300 nmol/L and 3.2 μmol/L, respectively, 4 h after addition, and high levels were retained at least to 20 h. Thus, the intracellular drug concentrations that induced mitotic arrest were equivalent for the two drugs (3.5 μmol/L for eribulin and 3.2 μmol/L for ER-076349) and these intracellular concentrations affected microtubule dynamics similarly. The extent of accumulation was greater for ER-076349 than for eribulin (150- and 800-fold for 2 and 4 nmol/L ER076349, respectively). With both drugs (eribulin and ER-076349), washing of the cells at 20 h and incubation in drug-free medium induced a rapid loss of drug from the cells, although less than half the intracellular eribulin was lost, whereas nearly all the intracellular ER-076349 was lost during the first hour after washing. Twenty-four hours after washing, intracellular concentrations of both drugs were equivalent to background (data not shown).

Discussion

We found that eribulin significantly suppressed centromere dynamics in mitotic spindles at drug concentrations that arrested mitosis, thus supporting the idea that suppression of spindle microtubule dynamics by eribulin is one of its major antiproliferative mechanisms. The mitotic spindle checkpoint delays anaphase until all chromosomes have properly attached to the spindle microtubules and become aligned at the metaphase plate (9). Passage through this checkpoint depends on tension at the kinetochores and

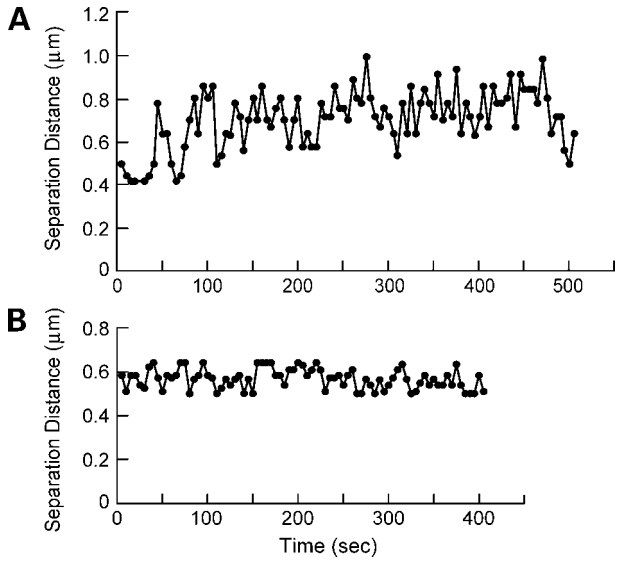

Figure 3. Time course of changes in the center-to-center separation distance between sister centromeres of a pair in the absence (top trace) and presence of 60 nmol/L eribulin (bottom trace). Images of GFP centromeres were collected from a single plane by confocal microscopy at 5 s intervals. Separation distances between the two members of pairs that remained well focused for the 7 min recording period were measured as described in Materials and Methods. For the centromere pair in the absence of drug, the centromeres were separated by 0.5 μm at zero time. The pair then underwent multiple episodes of stretching and relaxing. For example, at 45 s, the pair was separated by 0.79 μm; at 55 s, the separation distance decreased to 0.41 μm, the minimum separation observed for this pair; and at 275 s, it increased to 1.0 μm, the maximum separation observed for this pair. In the presence of 60 nmol/L eribulin, the separation distance was reduced overall and ranged from 0.73 to 0.28 μm for the centromere pair (*bottom*).

Table 1. Effects of eribulin and ER-076349 on centromere dynamics

Variable	Control	Eribulin, 30 nmol/L	Eribulin, 60 nmol/L	ER-076349, 2 nmol/L	ER-076349, 4 nmol/L
Rate of stretching (μm/min)	1.0 ± 0.4	1.3 ± 0.1	1.1 ± 0.1*	1.1 ± 0.1	1.0 ± 0.1
Rate of relaxing (μm/min)	1.4 ± 0.5	1.7 ± 0.1	1.1 ± 0.1*	1.6 ± 0.2	1.1 ± 0.1*
Duration of stretching (s)	12.7 ± 0.3	11.2 ± 0.5†	14.4 ± 0.9	11.0 ± 0.7†	10.6 ± 0.4†
Duration of relaxing (s)	12.5 ± 0.3	12.1 ± 0.4	13.9 ± 0.4*	11.5 ± 0.5	12.9 ± 0.4
Time stretching (%)	38 ± 2	28 ± 3.*	25 ± 2†	30 ± 2*	30 ± 5*
Time relaxing (%)	32 ± 2	26 ± 2†	24 ± 3‡	29 ± 3‡	24 ± 3‡
Time paused (%)	30 ± 3	46 ± 4†	50 ± 4†	40 ± 4*	46 ± 4†
Centromere dynamicity (μm/min)	0.84	0.79	0.55	0.80	0.57
Transition frequencies (events/min)	1.7	1.7	1.3	1.7	1.1
Mean separation (μm)	0.66 ± 0.11	0.69 ± 0.1	0.66 ± 0.15	0.70 ± 0.1	0.60 ± 0.1
Mean maximal separation (μm)§	0.96 ± 0.11	1.04 ± 0.11	0.87 ± 0.15	0.89 ± 0.12	0.88 ± 0.1
Mean minimal separation (μm)§	0.45 ± 0.12	0.43 ± 0.1	0.48 ± 0.09	0.47 ± 0.1	0.41 ± 0.1

NOTE: Between 6 and 11 pairs of centromeres from between 5 and 7 cells were measured for each condition.
*Significantly different from control values at the 95% confidence level (Student's *t* test).
†Significantly different from control values at the 98% confidence level (Student's *t* test).
‡Significantly different from control values at the 99% confidence level (Student's *t* test).
§The mean for all tracings of the two maximal separations (peaks) or the two minimal separations (valleys) during each 5-min tracing for each condition.

occupancy of kinetochores by an appropriate number of microtubules (8). Eribulin significantly reduced the rate of centromere relaxation and the percentages of time stretching and relaxing, increased the time that centromere pairs spent paused, neither stretching nor relaxing detectably, and reduced the transition frequency and the overall centromere dynamicity. For example, 2 × IC_{50} of eribulin (60 nmol/L) increased the percentage of time paused by 67% and decreased the centromere dynamicity by 35%. Thus, tension on the kinetochores was reduced, which in turn leads to prolonged metaphase arrest.

Eribulin, paclitaxel, and *Vinca* alkaloids bind differently to tubulin and/or microtubules. As shown by electron crystallography and three-dimensional reconstruction of microtubule protofilaments, paclitaxel binds along the inner surface of the microtubule with maximal binding of one paclitaxel molecule per tubulin heterodimer (17, 18), whereas vinblastine and eribulin bind with high affinity to a very small number of saturable sites on tubulin at the ends of the microtubule (19, 20).[3] The effects of binding of these drugs to microtubules vary. For example, the binding of one or two molecules of vinblastine to a microtubule end is sufficient to suppress microtubule treadmilling dynamics by 50% (20), whereas it requires paclitaxel occupancy of many more tubulin molecules in a microtubule to suppress microtubule dynamic instability by 50% (e.g., ~120 paclitaxel molecules bound along the inner surface of a microtubule of 5 μm length; ref. 17). Despite their chemical structural differences and their different binding modes on microtubules, these drugs at low concentrations all arrest mitosis by suppressing microtubule dynamics. The differences in the microtubule binding of eribulin, *Vinca* alkaloids, and paclitaxel make it unlikely that the drugs all sterically block interaction with the kinetochore. Their common feature is that they all suppress the stretching and relaxation movements between sister centromeres at concentrations that arrest mitosis, thus providing strong evidence that suppression of spindle microtubule dynamics by these chemically dissimilar molecules is their crucial antimitotic mechanism of action.

Absence of Reduction in Mean Centromere Separation Distance

The distance between sister centromeres and kinetochores has been used as an indicator of spindle-induced tension on kinetochores, a tension that is thought to play a role in signaling the metaphase/anaphase transition. Many microtubule-targeted drugs decrease the separation distance in association with mitotic arrest (12, 13, 21–23). Interestingly, at concentrations of eribulin and ER-076349 that induced significant mitotic arrest (1-2 × IC_{50}), there was no significant change in the mean centromere separation distance (Table 1). However, it is clear that at these concentrations, centromere dynamics were suppressed because the dynamicity and percentages of time stretching and relaxing were reduced (Table 1). The results suggest that a decrease in centromere separation is not a requirement for microtubule-targeted induction of mitotic arrest in bipolar spindles and that mean centromere separation may be only a crude measure of spindle tension. The kinetochore-microtubule interface is not static but fluid, and kinetochore components are dynamic (24). The dynamic push and pull of microtubules on kinetochore components must induce continuous changes in both the conformation of individual kinetochore protein components and the overall arrangement of the proteins within the kinetochore. The continuous and repetitive dynamic changes in the microtubule/kinetochore interface and within the kinetochore that are induced by microtubules

[3] J. Smith, L. Wilson, and M.A. Jordan, unpublished data.

pushing and pulling on the kinetochore may be essential for the biochemical alterations signaling the metaphase/anaphase transition and may be one of the important functions of dynamic microtubules in mitosis.

Eribulin Differs from Paclitaxel and Vinblastine in Its Specific Mechanistic Effects on Centromere Dynamics

Figure 5 compares the suppression of the variables of centromere dynamics in U-2 OS cells by eribulin with suppression by four major microtubule-targeted antimitotic drugs, vinblastine, vinorelbine, vinflunine, and paclitaxel (12, 13). The drug concentrations used were $\geq 2 \times IC_{50}$. All five drugs suppressed the relaxation rate, the percentage of time stretching and relaxing, the transition frequencies, and the overall dynamicity. In addition, they all increased the percentage of time paused. However, interestingly, unlike the other four drugs, eribulin did not suppress the stretching rate or duration or the relaxing duration. When centromere pairs stretch apart, the microtubules must be shortening (depolymerizing). Thus, this finding is consistent with the results obtained for eribulin *in vitro* with purified microtubules and in living interphase MCF7 cells (1). In these two systems, eribulin did not suppress the microtubule shortening rate or duration (which is associated with centromere stretching in the spindle) but primarily suppressed microtubule growth (associated with centromere relaxation in the spindle) and dynamicity. Thus, the results are consistent with a similar mechanism of action of eribulin on both interphase microtubule dynamics and mitotic spindle microtubule dynamics.

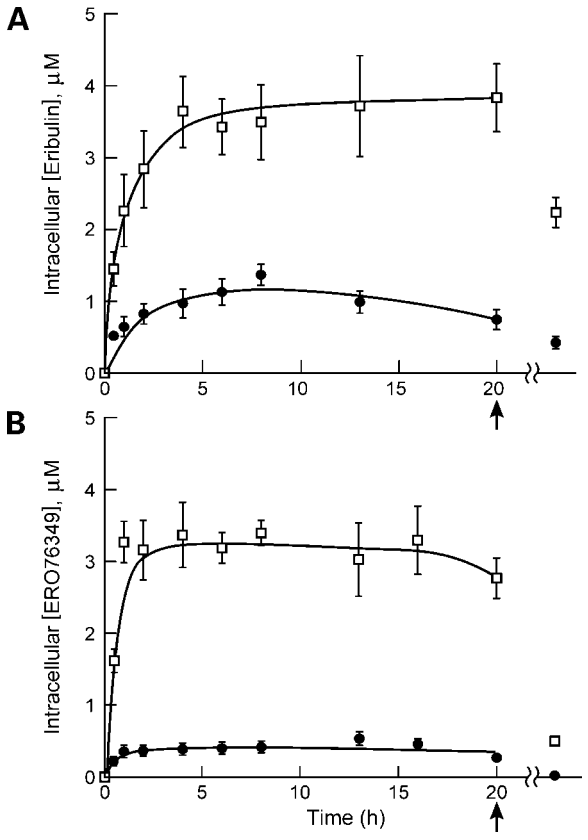

Figure 4. Time course of uptake of (**A**) [^{3}H]eribulin (*squares,* 60 nmol/L; *circles,* 30 nmol/L) and (**B**) [^{3}H]ER-076349 (*squares,* 4 nmol/L; *circles,* 2 nmol/L) into U-2 OS cells. [^{3}H]eribulin or [^{3}H]ER-076349 was added to U-2 OS cells growing exponentially (Materials and Methods). At time intervals from 30 min to 20 h, intracellular radioactivity was determined. After 20 h, cells were washed with 2 mL PBS and fresh medium was added (*arrow*) for 1 h (last data point) and for 24 h (data not shown) to determine radioactivity retained after washout. Mean and SE of five independent experiments.

Intracellular Levels of Eribulin and ER-076349

Although it required considerably higher concentrations of eribulin added to the medium than of ER-076349 to induce significant mitotic arrest ($2 \times IC_{50}$ was achieved at 60 nmol/L eribulin and 4 nmol/L ER-076349), the resulting effective intracellular concentrations of the two drugs were surprisingly similar (3.5 μmol/L eribulin and 3.2 μmol/L ER-076349). Thus, ER-076349 is preferentially taken up into the cells. Significantly, although their potencies differed 15-fold based on the drug concentration in the medium required for mitotic arrest, both compounds had similar effects on microtubule dynamic instability at the antimitotic concentrations, providing further strong evidence that effects on microtubule dynamic instability is a major mechanism underlying their ability to arrest mitosis.

The intracellular tubulin concentration is ~20 μmol/L (25), indicating that only a fraction of the cellular tubulin was bound to either drug at the concentrations that induced mitotic arrest. These results are in agreement with our previous results that eribulin appears to suppress microtubule dynamic instability by binding directly to a microtubule end.

In addition to a high extent of uptake of the C35-hydroxyl analogue ER-076349, it was taken up rapidly to equilibrium within 2 h and was lost very rapidly on washout, whereas the C35 amine compound eribulin required ≥4 h to reach equilibrium and was more difficult to wash out (Fig. 5). In breast, colon, ovarian cancer, and melanoma xenograft models, eribulin showed greater potency, efficacy, or both compared with ER-076349 despite the greater antiproliferative potency of ER-076349 in cell growth studies (Fig. 1; ref. 4). The finding here that ER-076349 is lost rapidly on washout, whereas eribulin is retained to a greater extent may explain, at least in part, the relative irreversibility of mitotic blocks by eribulin and its enhanced *in vivo* efficacy (4).

Conclusion

Eribulin is chemically distinct from the microtubule-targeted drugs paclitaxel and *Vinca* alkaloids; it binds differently to microtubules than paclitaxel and it suppresses microtubule dynamics in a distinct manner from paclitaxel and *Vinca* alkaloids. However, at concentrations that induce mitotic arrest, all of these drugs suppress centromere dynamics. These results provide strong support for the idea that suppression of spindle microtubule dynamics by these drugs and the resulting disruption of tension on the chromosome kinetochores/centromeres is the primary mechanism responsible for their abilities to induce mitotic arrest.

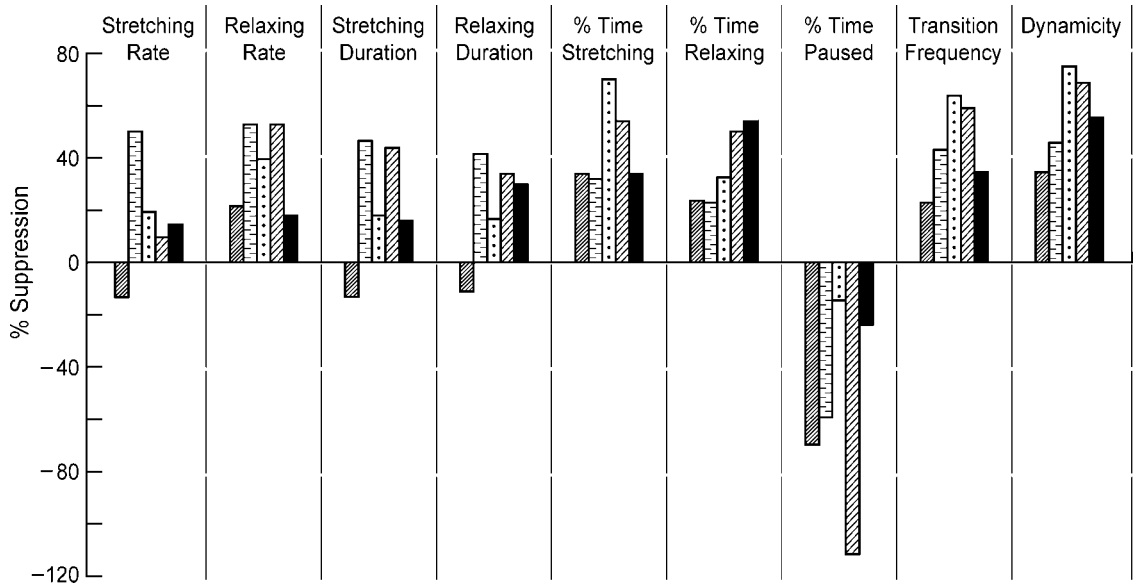

Figure 5. Histogram comparing the percent suppression of the major variables of centromere dynamics in U-2 OS cells by eribulin (60 nmol/L, *left, dark hatched columns*) with those found previously to be induced by vinblastine (50 nmol/L, *interlaced hatched columns*), vinorelbine (50 nmol/L, *dotted columns*), vinflunine (50 nmol/L, *light hatched columns*; ref. 13), and paclitaxel (100 nmol/L, *solid columns*; ref. 12). The drug concentrations were all $\geq$2 times the concentration that induced half-maximal mitotic arrest to ensure that the observed suppression was associated with significant mitotic arrest. Specifically, the concentrations were 2 $\times$ IC_{50}, 8 $\times$ IC_{50}, 7 $\times$ IC_{50}, 3 $\times$ IC_{50}, and 2 $\times$ IC_{50}, respectively.

Disclosure of Potential Conflicts of Interest

B.A. Littlefield: Eisai Research Institute employee; T. Okouneva, O. Azarenko, L. Wilson, and M.A. Jordan received grant support from Eisai Research Institute.

References

1. Jordan MA, Kamath K, Manna T, et al. The primary antimitotic mechanism of action of the synthetic halichondrin E7389 is suppression of microtubule growth. Mol Cancer Ther 2005;4:1086 – 95.

2. Dabydeen D, Burnett J, Bai R, et al. Comparison of the activities of the truncated halichondrin B analog NSC 707389 (E7389) with those of the parent compound and a proposed binding site on tubulin. Mol Pharmacol 2006;70:1866 – 75.

3. Kuznetsov G, Towle MJ, Cheng H, et al. Induction of morphological and biochemical apoptosis following prolonged mitotic blockage by halichondrin B macrocyclic ketone analog E7389. Cancer Res 2004;64: 5760 – 6.

4. Towle MJ, Salvato KA, Budrow J, et al. *In vitro* and *in vivo* anticancer activities of synthetic macrocyclic ketone analogs of halichondrin B. Cancer Res 2001;61:1013 – 21.

5. Shelby RD, Hahn KM, Sullivan KF. Dynamic elastic behavior of α-satellite DNA domains visualized *in situ* in living human cells. J Cell Biol 1996;135:545 – 57.

6. Skibbens RV, Skeen VP, Salmon ED. Directional instability of kinetochore motility during chromosome congression and segregation in mitotic newt lung cells: a push-pull mechanism. J Cell Biol 1993;122: 859 – 75.

7. Li X, Nicklas RB. Mitotic forces control a cell-cycle checkpoint. Nature 1995;373:630 – 2.

8. Nicklas RB, Waters JC, Salmon ED, Ward SC. Checkpoint signals in grasshopper meiosis are sensitive to microtubule attachment, but tension is still essential. J Cell Sci 2001;114:4173 – 83.

9. Pinsky BA, Biggins S. The spindle checkpoint: tension versus attachment. Trends Cell Biol 2005;15:486 – 93.

10. King JM, Nicklas RB. Tension on chromosomes increases the number of kinetochore microtubules but only within limits. J Cell Sci 2000;113: 3815 – 23.

11. Nicklas RB, Ward SC. Elements of error correction in mitosis: microtubule capture, release, and tension. J Cell Biol 1994;126: 1241 – 53.

12. Kelling J, Sullivan K, Wilson L, Jordan MA. Suppression of centromere dynamics by Taxol in living osteosarcoma cells. Cancer Res 2003;63:2794 – 80.

13. Okouneva T, Hill BT, Wilson L, Jordan MA. The effects of vinflunine, vinorelbine, and vinblastine on centromere dynamics. Mol Cancer Ther 2003;2:427 – 36.

14. Littlefield BA, Palme MH, Seletsky BM, et al. Macrocyclic analogs and methods of their use and preparation. U.S. Patent 6214865; 2001.

15. Kamath K, Jordan MA. Suppression of microtubule dynamics by epothilone B in living MCF7 cells. Cancer Res 2003;63:6026 – 31.

16. Toso RJ, Jordan MA, Farrell KW, Matsumoto B, Wilson L. Kinetic stabilization of microtubule dynamic instability *in vitro* by vinblastine. Biochemistry 1993;32:1285 – 93.

17. Derry WB, Wilson L, Jordan MA. Substoichiometric binding of Taxol suppresses microtubule dynamics. Biochemistry 1995;34:2203 – 11.

18. Nogales E, Wolf SG, Khan IA, Luduena RF, Downing KA. Structure of tubulin at 6.5A and location of the Taxol-binding site. Nature 1995;375: 424 – 7.

19. Jordan MA, Wilson L. Kinetic analysis of tubulin exchange at microtubule ends at low vinblastine concentrations. Biochemistry 1990; 29:2730 – 9.

20. Wilson L, Jordan MA, Morse A, Margolis RL. Interaction of vinblastine with steady-state microtubules *in vitro*. J Mol Biol 1982;159:129 – 49.

21. Waters JC, Chen R-H, Murray AW, Salmon ED. Localization of Mad2 to kinetochores depends on microtubule attachment, not tension. J Cell Biol 1998;141:1181 – 91.

22. Rathinasamy K, Panda D. Suppression of microtubule dynamics by benomyl decreases tension across kinetochore pairs and induces apoptosis in cancer cells. FEBS J 2006;273:4114 – 28.

23. Skoufias DA, Andreassen P, Lacroix F, Wilson L, Margolis RL. Mammalian mad2 and bub1/bubR1 recognize distinct spindle-attachment and kinetochore-tension checkpoints. Proc Natl Acad Sci U S A 2001;10: 4492 – 7.

24. Maiato H, DeLuca J, Salmon E, Earnshaw W. The dynamic kinetochore-microtubule interface. J Cell Sci 2004;117:5461 – 77.

25. Jordan MA, Thrower D, Wilson L. Mechanism of inhibition of cell proliferation by *Vinca* alkaloids. Cancer Res 1991;51:2212 – 22.